Multimedia Tools and Applications
https://doi.org/10.1007/s11042-022-11932-1

A new automated segmentation and classification of mammogram images

Rajeshwari S. Patil, et al. *[full author details at the end of the article]*

Received: 19 July 2021 / Revised: 18 November 2021 / Accepted: 3 January 2022
Published online: 28 January 2022

Abstract
Early-stage recognition of lesions is the better probable manner for fighting against breast cancer to find a disease with the highest ratio of malignancy around women. Existing approaches are generally based on deep learning that has been designed for the segmentation of tumors, however, it is complex because of the false positives and the inaccurate detection of boundaries for segmentation, as the existing models incorrectly predict the positive classes, thus affecting the overall classification. In this paper, an enhanced mammogram image classification is proposed by introducing novel segmentation and classification approaches. The initial process of the proposed model is pre-processing, which is performed by the median filtering that tends to remove the noise from the images. The preprocessed images are subjected to segment the tumor from the mammogram images by a new segmentation approach termed Region growing with Adaptive Fuzzy C-Means Clustering (RG-AFCM). Once the segmentation of the tumor is done, feature extraction is performed, where the features are extracted using Gray-Level Run-Length Matrix (GLRM) and Grey Level Co-occurrence Matrix (GLCM) approaches. Furthermore, the extracted features are classified using optimal trained Recurrent Neural Networks (RNN). Here, a new algorithm named Average Fitness New Updating-based Grasshopper Optimization Algorithm (AFU-GOA) is proposed for enhancing both the segmentation and classification phases. Finally, the performance of RG-AFCM-based segmentation is compared over the stat-of-the-art segmentation approaches, and optimal trained RNN is compared over the existing classifiers and deep learning models to prove the reliability of the proposed model. The accuracy of the developed AFU-GOA-RNN is 1%, 2%, 1%, and 3% enhanced than PSO-RNN, GWO-RNN, FF-RNN, and GOA-RNN. Hence, the proposed classification using AFU-GOA-based trained RNN establishes a better performance than existing models.

Keywords Mammogram image processing · Region growing with adaptive fuzzy C-means clustering · Optimal trained recurrent neural networks · Average fitness-based new updating based grasshopper optimisation algorithm

1 Introduction

One of the major types of cancer is breast cancer among women around the world. Early identification of breast cancer is important for successful treatment and minimization of mortality rate [46]. Among traditional diagnostic modalities, the bio-specimen-based test remains the best standard for deciding whether a breast lump is benign or malignant [8]. Though, around 10–31% of the breast lumps are considered as the surgical biopsy that is turned into a malignant [15]. The majority of the false-positive biopsies are redundant and could be possibly avoided through a much consistent breast cancer screening approach. Recent advancements in the medical imaging approaches such as tomosynthesis, Magnetic Resonance Imaging (MRI), ultrasound, and mammography have been developed in a medical environment for breast cancer detection at an early stage [3]. The implementation of a CAD model for assisting radiologists in the detection and classification of breast cancer has been studied in the literature. The (Computer-Aided Diagnosis)CAD model is a type of semi-automatic or automatic tool implemented for assisting radiologists in the detection and classification of mammographic abnormalities [43].

The effectiveness of a CAD is based on improving accuracy through the proper segmentation of the tumors in mammograms [44]. Therefore, the segmentation of mammogram images is a significant process to diagnose tumors as malignant and benign. Image segmentation has a major role that separating an image into sub-parts of diverse clusters. It is the procedure of discovering the groups of pixels in mammogram images [39] [17]. Different image segmentation techniques are proposed in the literature that is categorized as energy function-based methods, clustering methods, contour-based techniques, region-based techniques, and thresholding techniques, which are classified based on either supervised or unsupervised methods. Initially, the data of classes are described in advance while there is no requirement of defining it in the unsupervised classification process [13]. Additionally, there are two categories of clustering in a pixel-based approach that are fuzzy and hard clustering [10]. The major part of the segmentation of the medical image is to distinguish the anatomical characteristics and split the component of interest like glands, tumors, and fibroids from the background of the image [28]. However, it faces a few challenges like poor resolution and contrast weakness. These limitations have arrived from the existence of artifacts that are arrived based on the movement of patient and noise of instrumental problem [17]. The motivation of the proposed model is to propose a new breast cancer detection model that can handle some hard and challenging, large-scale optimization [21] problems and less convergence rate. The real-world applications of the proposed model are listed given below, bus schedules, traffic lights, duplicating outcomes, google search, facial recognition, sorting papers.

Perfect detection of suspicious breast lesions plays a significant role in attaining a high (True Positive Rate)TPR to improve the final diagnosis of breast cancer [33]. Breast lesions detection is crucial due to the dependency of variables concerned with shape, size, texture, and location. It is done by developing some technologies like machine learning and image processing approaches [2]. These existing approaches are based on the handcrafted features, low-level and it also requires the capability for performing the detection task in an automatic manner [19]. In recent years, new deep learning approaches have been offered for overcoming the bad detection performance on CAD models [34]. The classification of breast lesions is the last phase of CAD models. The major goal of this phase is to distinguish the detected breast lesion as either malignant or benign. The ability of the classification procedure is especially based on the effectiveness of the specific feature, which represents the major properties of breast lesions [27]. Based on the better characteristic distributions of the deep features, the recognition of malignant and benign breast lesions is determined to improve efficiency [42]. The major contribution of this proposed breast cancer detection model is to gather data from a standard dataset called MIAS mammography for evaluating the performance of the proposed model by comparing it with diverse segmentation, heuristic, and machine learning approaches. To improve the segmentation accuracy using RG-AFCM, the proposed AFU-GOA aims to optimize the threshold value in RG-AFCM. To classify the extracted features using AFU-GOA-trained RNN to get optimal classes like normal, malignant, and benign. A new AFU-GOA technique is proposed for the optimization of threshold in the segmentation stage and the optimization of weight updating in the classification stage.

The remaining sections of this paper are listed here. Section II explains the related works. Section III discusses the development of mammogram image classification for breast cancer detection by an enhanced segmentation approach. Section IV depicts RG-AFCM-based segmentation for breast cancer detection. Section V explains AFU-GOA-trained RNN for mammogram image classification. Section VI discusses results. Section VII concludes this paper.

1.1 Literature survey

1.1.1 Related works

In 2014, Dheeba et al. [6] have developed a new classification model to detect the abnormalities of the breast in digital mammograms through (Particle Swarm Optimized Wavelet Neural Network)PSOWNN. This algorithm was performed based on the extraction of "Laws Texture Energy" metrics from the mammograms and classification of the suspicious regions was done through a pattern classifier. It was performed on a "real clinical database of 216 mammograms" taken from mammogram screening centers.

In 2017, Duraisamy and Emperumal [7] have developed a new deep learning-based model for the classification of digital mammograms. The advancement of this approach was based on the tumor tissues along with the level sets. It was complex for segmenting the mammogram image because of the low distinction among normal and lesion tissues. Thus, (Chan-Vese)C-V level set approach has been employed for extracting the original contour of mammograms. Moreover, (Deep Learning Convolutional Neural Network)DL-CNN technique was applied for learning the features of microcalcification clusters and mammary-specific mass. In the DL-CNN network, an eminent fully complex-valued relaxation network classifier was employed at the last phase for increasing the accuracy of a classification and reducing the false positives.

In 2020, Mugahed et al. [24] have researched and incorporated a CAD model based on detection using deep learning and classification, which was aimed at improving the performance of diagnostic of breast lesions. Initially, a deep learning YOLO detector was applied and analyzed for the detection of breast lesions from whole mammograms. Moreover, the classifiers like InceptionResNet-V2, ResNet-50, and regular feedforward CNN were altered and calculated for the classification of breast lesions. The implemented deep learning model was analyzed on 5-fold cross-validation tests with two diverse and broadly employed "databases of digital X-ray mammograms such as DDSM and INbreast".

In 2019, Vijayarajeswari et al. [40] have offered a model for the classification of mammograms by applying Hough transform features. This Hough transform was employed for isolating the feature of a specific shape in an image. The early diagnosis of breast cancer was significantly performed with the mechanized identification of masses and characterization of miniaturized scale. The feature extraction [38] approach called Hough transform was applied in this research model for detecting the features from mammogram images.

In 2019, Kaura et al. [16] have consisted of a novel method that was applied on the “Mini-MIAS dataset of 322 images”. This research model has involved stages like “pre-processing, feature extraction, and classification”. The feature extraction process was employed by K-mean clustering to select (Speed-Up Robust Features)SURF. In the classification process, a new layer was inserted that has used approaches like (Deep Neural Network)DNN and (Multiclass Support Vector Machine)MSVM. The result has established an enhanced accuracy rate through MSVM and DNN. Moreover, the research model has also attained better accuracy with all three classes like normal, malignant, and benign cancer.

In 2019, Salih and kamil [36] have offered an approach for segmenting the boundary of breast masses regions in mammograms using a developed technique based on fuzzy set approaches. Initially, the research model was executed on mini-MIAS for evaluating the research algorithm. The dataset was pre-processed for removing the noise. Furthermore, a fuzzy set with a fuzzy inference model was employed for the research model for produced two input parameters. These features were filtered using the thresholding filter.

In 2019, Muduli et al. [23] have implemented an enhanced CAD system to classify the breast masses into abnormal or normal and malignant or benign classes. The developed system has employed (Lifting Wavelet Transform)LWT for extracting the features from the ROI mammogram images. Further, the dimensionality of the feature vectors was minimized through approaches like (Linear Discriminant Analysis)LDA and (Principal Component Analysis)PCA. Lastly, an integrated approach called MFO-ELM was applied for classification. Here, the hidden node parameters of (Extreme Learning Machine)ELM were optimized using (Moth Flame Optimization)MFO. Moreover, the generalization performance was improved by applying 5-fold stratified cross-validation. The implemented system was executed on “two standard datasets, namely MIAS and DDSM”.

In 2019, Zheng et al. [47] have developed a model called DLA-EABA for detecting breast cancer using improved computational approaches, where the tumor classification approach has been employed with the transfers by utilizing the deep CNNs concept. Initially, CNN-based transfer learning was examined for characterizing the breast masses to diverse prognostic or predictive tasks or diagnostic or in different imaging modalities like tomosynthesis, US, mammography, MRI, and digital breast. The deep learning structure has consisted of numerous Max-pooling layers, (Long Short-Term Memory)LSTM, and convolutional layers. The error estimation and classification have been contained in a softmax layer and fully connected layer.

1.1.2 Problem statement

The segmentation procedure has limitations such as poor resolution and contrast weakness. Some of the segmentation approaches to research in the literature are C-V level set segmentation, Fuzzy set, and intensity-based segmentation approach. The challenges present in the above-mentioned techniques are given here. C-V level set segmentation approach requires more numerical stability. Though, the computation of all image data and computing time are unbearable at every iteration. Similarly, due to the higher-order logic, the implementation of a fuzzy set is difficult. The suspected breast cancer has appeared as white spots in mammography images. The sensitivity of mammography is influenced by factors like the pectral muscle, breast density, artifacts or even the presence of tags. Therefore, for solving these challenges, many approaches have been listed in literature that has diverse challenges and features. PSOWNN [6] achieves better classification accuracy and enhances convergence behavior. Though, it is not suitable for detecting the masses. DL-CNN algorithm and C-V level set segmentation [7] is research for enhancing the accuracy of classification. It has better AUC score. On the other hand, this is not applicable for standard databases and larger architectures. Ensemble learning [24] improves overall accuracy and enhances the performance of diagnostic. However, there is less number of standard datasets. SVM(Support Vector Machine) with intensity-based segmentation [22, 40] efficiently classifies the abnormal classes and attains better accuracy of classification. Conversely, it doesn't perform well on classification with diverse classes. The challenges for deep learning algorithms [5, 35] are listed given below, it requires large amounts of data. Furthermore, the more powerful and accurate models will need more parameters, which, in turn, require more data [14, 20]. Once trained, deep learning models become inflexible and cannot handle multitasking, and also they obtain low accuracy. For these disadvantages, the deep learning algorithms gave bad results compared with the other existing heuristic algorithms. The accuracy of the designed MAE-EFO-I-DNN is 43%, 24%, 21%, 9.5%, and 8% enhanced than DT, SVM, KNN, and DNN, respectively. From the above result analysis, they have proved that the DNN attained lower performance than the other algorithms. K-mean clustering with MSVM [16] is developed for improving accuracy and effectively pre-processes the images. Though, this model is not applied on large-scale network. Fuzzy logic with Fuzzy set segmentation [36] improves the diagnosis process and minimizes the false positive detection. On the other hand, when the rules of fuzzy systems are flawed, then the outcomes may not be suitable. MFO-ELM algorithm [23] improves accuracy and reduces the computational time. Though, this model influences on performance due to the stochastic nature of this algorithm. DLA-EABA [47] enhances accuracy and specificity and obtains high performance. However, it attains more false positives. The computation time is low and it does not use for larger datasets. In our proposed model, based on the comparative analysis the computation time is better than the other algorithms, and also the larger datasets have been used to show the performance of the proposed model. Thus, these challenges are considered to implement a new model of mammogram images with segmentation and classification along with a deep learning model. The review of the traditional diverse mammogram image classification models is given in Table 1.

2 Development of mammogram image classification for breast cancer detection by enhanced segmentation approach

2.1 Proposed architecture

Image segmentation is the major challenging issue in image processing nowadays. Similarly, it is also the active research and challenging point filed in the area of medical image processing. Segmentation of mammogram images is challenging work and there are a requirement and wide scope for future research for improving the precision, accuracy, and speed of the segmentation process. The major challenges for the proposed segmentation approach such as inadequate resolution, less segmentation accuracy, detection of linear structures, and differentiation of thin structures are observed in mammogram image segmentation. By considering the abovementioned problems, it is required to propose a novel segmentation approach for discovering tumors and its tissues classification to detect the abnormalities in

Table 1 Review of traditional diverse Mammogram Image classification models

Author [citation]	Methodology	Features	Challenges
Dheeba et al. [6]	PSOWNN	• It achieves better classification accuracy. • It enhances convergence behaviour.	• Though, it is not suitable for detecting the masses.
Duraisamy and Emperumal [7]	DL-CNN algorithm	• It enhances accuracy of classification. • It has better AUC score.	• It is not applicable for standard databases and larger architectures.
Mugahed et al. [24]	Ensemble learning	• It improves overall accuracy. • It enhances the performance of diagnostic.	• However, there is less number of standard datasets.
Vijayarajeswari et al. [40]	SVM	• It efficiently classifies the abnormal classes. • It attains better accuracy of classification.	• It doesn't perform well on classification with diverse classes.
Kaura et al. [16]	K-mean clustering with MSVM	• It improves better accuracy. • It effectively pre-processes the images.	• This model is not applied on large-scale network.
Salih and kamil [36]	Fuzzy logic	• The diagnosis process is improved. • It minimizes the false positive detection.	• When the rules of fuzzy systems are flawed, then the outcomes may not be suitable.
Muduli et al. [23]	MFO-ELM algorithm	• It improves accuracy. • It reduces the computational time.	• It influences on performance due to the stochastic nature of this algorithm.
Zheng et al. [47]	DLA-EABA	• It enhances accuracy and specificity. • It obtains high performance.	• However, it attains more false positives.

breast cancer at an earlier stage. The challenging of classification is listed given below, **Intra-Class Variation, Scale Variation, View-Point Variation, Background Clutter.** By considering the abovementioned problems to classify the extracted features using AFU-GOA-trained RNN to get optimal classes like normal, malignant, and benign, where the weight is updated using this proposed algorithm. New progressions in the area of machine learning with extensive and deeper representation techniques, generally named as deep learning methods offer more remarkable influence on enhancing the capabilities of diagnostics in the CAD models. Therefore, there is a huge demand on developing a detection of segmenting and classifying the breast cancer mammogram images. The proposed detection model is represented in Fig. 1.

The proposed model intends to develop a new segmentation and classification model for mammogram images in breast cancer using different phases like "data collection, preprocessing, segmentation, feature extraction, and classification." The data is gathered from standard dataset called MIAS Mammography. The gathered data is preprocessed using median filtering. Preprocessing is the process of reducing the false positive rates and limiting the analysis of abnormalities without unnecessary influence from background of the mammogram images. Further, the preprocessed images are subjected to the enhanced tumor segmentation approach called RG-AFCM, in which the AFU-GOA is employed for optimizing threshold to choose the accurate region in clustering. Segmentation is the process of extracting an (Region of Interest)ROI to provide an exact measurement of breast regions via normal and abnormalities

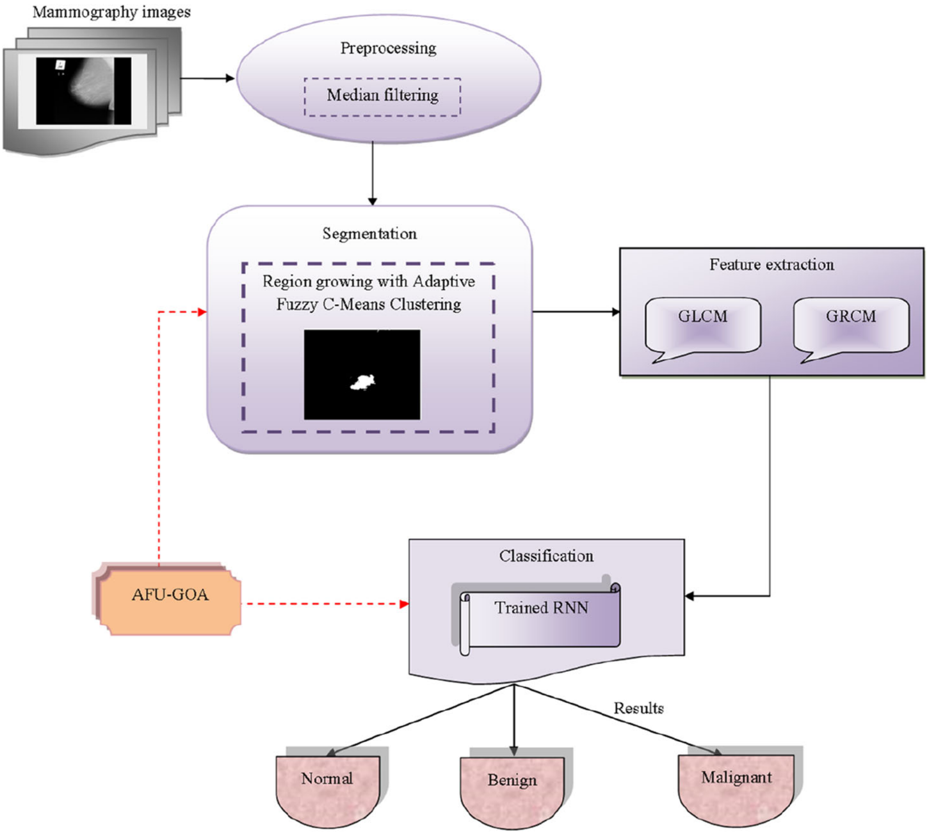

Fig. 1 Proposed segmentation and classification of mammogram images

regions. The segmented images are further given to the feature extraction process for selecting the significant features, which is done by applying the GLCM and GRCM. The extracted features are classified using AFU-GOA-trained RNN, in which the weight of RNN is updated through the same proposed AFU-GOA. This algorithm is developed based on the average fitness-based new updating procedure in the GOA. The proposed model efficiently classifies the outcomes as normal or malignant or benign. Moreover, the proposed model aims to maximize the accuracy of segmentation and classification by the optimal model.

2.2 Dataset description

The proposed model gathers data from a standard dataset called MIAS Mammography, which is collected from https://www.kaggle.com/kmader/mias-mammography:Accessdate: 2020-11-17 . This dataset consists of annotations or labels and images for scans of mammography. It contains 7 columns with diverse information like "reference number, character of background tissue, class of abnormality present, severity of abnormality, image-coordinates of centre of abnormality, and approximate radius of a circle enclosing the abnormality". It includes 322 image files, where Benign has 207 images, normal type consists of 64 images and malignant type has 51 images. All the images in the dataset have the size of 1024 pixels × 1024 pixels. The sample images considered for the experimentation is given in Fig. 2.

Type of images	Sample image 1	Sample image 2
Benign	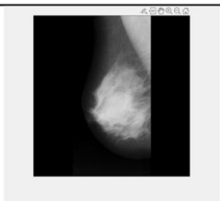	
Normal	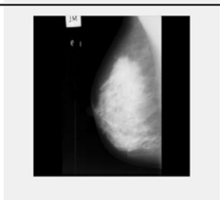	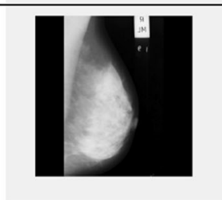
Malignant	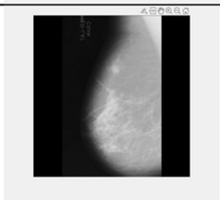	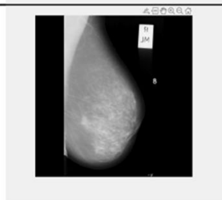

Fig. 2 Sample mammography images from MIAS mammography dataset

2.3 Image pre-processing

It is the initial stage in the proposed segmentation and classification model of mammogram images. Preprocessing is necessary for improving the quality of image and provides more precise segmentation and classification outcomes. Initially, this stage removes the artifact and unnecessary components in the background of mammogram images. It is also intended for improving the image appearance to eradicate error or noise or to emphasize specific features in mammogram. The proposed model uses median filtering [48] as the preprocessing approach, which is a non linear filter. It is an efficient approach for eliminating the salt and pepper noise, which aims for preserving the sharpness of image edges when eliminating noise. Here, the proposed model choose median filter because of the features like simple implementation and more robustness. It is essential due to the complex interpretation of mammogram images. This median filter is aimed to reduce the quantity of intensity differentiation among one pixel and the others. The noise difference of the median filtering is approximately computed for an image through zero mean noise below normal distribution, which is given in Eq. (1).

$$\boldsymbol{In}_{tm}^{im(pre)}(x,y) = \boldsymbol{median}\left\{\boldsymbol{In}_{tm}^{im}(x-t,y-u)t,u \in M\right\} \tag{1}$$

Here, the input mammogram images are termed as $\boldsymbol{In}_{tm}^{im}$, where $tm = 1, 2, \cdots, TM$and TMindicates total images in the dataset Mdenotes the 2D-mask and the preprocessed image is denoted as$\boldsymbol{In}_{tm}^{im(pre)}$.

3 Region growing with adaptive fuzzy C-means clustering-based segmentation for breast cancer detection

3.1 Enhanced tumor segmentation

The proposed model implements the enhanced tumor segmentation using RG-AFCM approach, which is the combination of region growing and AFCM techniques. Segmentation is an essential process to detect abnormal tissues in the breast that requires being more accurate. It helps to categorize the breast regions as normal and abnormal as well. It works for unraveling the breast regions from the other objects or from the background. It is required for preserving the margin characteristics of mammograms prior to any additional processing. Moreover, the segmentation aims to alter the depictions of an image into specific that is more significant and simpler to analyze. The enhanced RG-AFCM first performs the optimized region growing. Here, $\boldsymbol{In}_{tm}^{im(pre)}$is given as input. The optimized RG is the customized version of single seed RG technique. It is generally employed for diverse image segmentations. It works by the group of pixels into regions of image that is performed with a seed pixel and then connects the pixels of homogeneous until it satisfies the segmentation. Consider Oas the whole area of input$\boldsymbol{In}_{tm}^{im(pre)}$ that is separated into $\boldsymbol{or}$sub-regions$O_1, O_2, \cdots, O_{\boldsymbol{or}}$. $O_1, O_2, \cdots, O_{\boldsymbol{or}}$. Further, it should satisfy the following rules in the region growing approach that is described below. The pseudocode for the RG-AFCM model is described given below in Algorithm 1.

Step 1: $\cup_{v=1}^{\boldsymbol{or}} O_{\boldsymbol{or}} = O$;
Step 2: For$O_1, O_2, \cdots, O_{\boldsymbol{or}}$, the connected region is represented as$O$.
Step 3: For any$v, z, v \neq z, O_v \cap O_z = \alpha$;
Step 4: $GV(O_v) = \boldsymbol{true}$;
Step 5: $O(O_v \cup O_z) = \boldsymbol{false}$;

Algorithm 1: RG-AFCM model	
Step 1	Read the preprocessed images.
Step 2	Perform region growing method to update threshold using proposed AFU-GAO.
Step 3	The outcome of region growing has to send through Fuzzy C means Clustering.
Step 4	Compute the membership matrix it is represented as a matrix μ_{cldp} using the centroid pr_{cl}.
Step 5	Check with a threshold to find the segmented results of AFU-GAO.
Step 6	Final segmented images are represented as $In_{tm}^{im(seg)}$.

Here, the term$GV(O_v)$denotes the grey level value of the set$O_v$and $\boldsymbol{or}$represents the entire sum of pixels of an image. Initially, it selects seed points and the average of the imageav is formulated in Eq. (2).

$$av = \frac{1}{\boldsymbol{or}} \sum_{(t,u)\in O} Ve(t,u) \tag{2}$$

$$|Ve(t,u) - av|_{(t,u)\in O} < Thr_{RG} \tag{3}$$

Here, the value at the coordinate (t, u) is denoted as $Ve(t, u)$, the threshold or tolerance that should be very close to the average of an image is termed as Thr_{RG}. The performance of segmentation is improved by the selection of seed and threshold in this region growing approach. Here, the threshold is optimized using the proposed AFU-GOA to achieve the more precise segmentation. By considering the optimized threshold value, the optimal regions are segmented that is denoted as $\boldsymbol{In}_{tm}^{im(RG)}$. The obtained images $\boldsymbol{In}_{tm}^{im(RG)}$ are given to the AFCM approach to attain final segmented images. This AFCM is an extended version of FCM, in which the threshold is fixed for selecting the most optimal cluster. The proposed AFU-GOA helps in optimizing this threshold value, so that the cluster centroid that is very nearer to the threshold is selected as the final cluster. FCM [1] is a type of fuzzy clustering method. It works by minimizing the quadratic condition, in which the clusters are specified through its specific centers. Assume a set of Dp data patterns of $\boldsymbol{In}_{tm}^{im(RG)}$ as $Ps = \{ps_1, ps_2, \cdots, ps_{Dp}\}$, which permits for partitioning the data spaces through computing the centers of classes cc and MU denotes the membership matrix. The minimization of objective function Ob_{fcm} in terms of its centers and membership degrees is equated in Eq. (4).

$$Ob_{fcm} = \sum_{cl=1}^{CU} \sum_{dp=1}^{Dp} \mu_{\boldsymbol{cldp}}^{rn} \left\| ps_{dp} - pr_{cl} \right\|^2 \tag{4}$$

In Eq. (4), the number of patterns is termed as Dp, the number of clusters is specified as CU, and any real number is indicated as rn. Moreover, the degree of fuzzy membership is noted as $\mu_{\boldsymbol{cldp}}$ of pixel ps_{dp} in the cl^{th} cluster, the cluster center is termed as pr_{cl} in the cl^{th} cluster and the similarity measure is specified as $\| \|$. The objective function is reduced when assigning the huge membership values to input patterns, which are closer to its adjacent cluster centers. Further, it allocates the low membership values when it is distant from the cluster centers. Compute the membership matrix $\mu_{\boldsymbol{cldp}}$ using the centroid pr_{cl} as given in Eq. (5).

$$\mu_{\boldsymbol{cldp}} = \frac{1}{\sum_{cl=1}^{CU} \left[\frac{\left\| ps_{dp} - pr_{cl} \right\|^{\frac{2}{rn-1}}}{\left\| ps_{dp} - pr_{cl} \right\|^{\frac{2}{rn-1}}} \right]} \tag{5}$$

Compute centroid by in Eq. (6).

$$pr_{cl} = \frac{\sum_{dp=1}^{Dp} \mu_{\boldsymbol{cldp}}^{rn} ps_{dp}}{\sum_{dp=1}^{Dp} \mu_{\boldsymbol{cldp}}^{rn}} \tag{6}$$

Here, the clusters are selected as $cl = 1, 2, \cdots, CU$, where CU is fixed as 3 in the proposed model. As mentioned earlier, a threshold $Thr_{\boldsymbol{AFCM}}$ is assigned for improving the FCM segmentation, which is optimized by the proposed AFU-GOA. Here, 3 clusters are obtained from the FCM clustering, from which the centroid value in each cluster is checked with the optimized threshold. The cluster centroid closer to the threshold is selected as the optimal cluster, which is considered as the final segmented images $\boldsymbol{In}_{tm}^{im(seg)}$. The detailed representation of proposed AFU-GOA-RG-AFCM segmentation is given in Fig. 3.

3.2 Proposed algorithm

A new AFU-GOA is utilized in the segmentation and classification stages of proposed breast cancer detection, which enhances the RG-AFCM-based segmentation and training of RNN. This algorithm is developed from conventional GOA. It is applied for resolving the structural optimization problems, which is motivated from the hunting behavior of grasshopper swarms towards their food. It has the ability to solve the real time problems with unknown search spaces. It is a type of insects that is combined with the largest swarm of all non-human beings. The unique character of grasshopper swarm is the spilling over activities that are represented in adulthood and nymph stages. The swarm movement of grasshopper in nymph stage is less. The food resource seeking nature is one of the major features of grasshopper. There are two phases in this optimization algorithm that are “exploration and exploitation”. The quick movement of search agents is determined in the exploration and the movement is done locally in the exploitation phase. By considering these two tasks, the food resource seeking is mathematically formulated here.

$$A_x = S_x + F_x + W_x \tag{7}$$

$$S_x = \sum_{\substack{y=1 \\ y \neq 1}}^{N} s(d_{xy})\hat{d}_{xy} \tag{8}$$

$$F_x = -b\hat{e}_b \tag{9}$$

$$W_x = d\hat{e}_{wr} \tag{10}$$

Here, the position of the x^{th}grasshopper is termed asA_x, the term $S_x$indicates social interaction, gravity force on the x^{th}grasshopper is denoted asF_x and wind advection is specified asW_x. Random behavior of Eq. (7) is formulated as$A_x = r1S_x + r2F_x + r3W_x$, in which the random numbers are indicated as$r1$,$r2$, and$r3$that are in the range of [0, 1]. Additionally, the space among thex^{th}grasshopper and y^{th}grasshopper is specified asd_{xy}, where$d_{xy} = |a_x - a_y|$, and a unit vector is shown as$\hat{d}_{xy} = \frac{a_y - a_x}{a_{xy}}$ from the x^{th}grasshopper to the y^{th}grasshopper, the constant drift is noted as $d$and in the direction of wind a unity vector is termed as$\hat{e}_{wr}$. The gravitational constant is noted as $b$and a unity vector in the direction to the centre of earth is specified as$\hat{e}_b$, the term Nshows the number of grasshoppers and social forces termed as $s$is represented in Eq. (11).

$$s(r) = ge^{\frac{-r}{f}} - e^{-r} \tag{11}$$

The attractive length scale is termed as$f$and the intensity of attraction is noted as$g$. At larval phase, the Grasshoppers have no wings; consequently its movements are mostly correlated in the direction of wind. By expanding this Eq. (9), the components are substituted as derived in Eq. (12).

$$A_x = \sum_{\substack{y=1 \\ y \neq 1}}^{N} s(|a_x - a_y|)\frac{a_y - a_x}{a_{xy}} + -b\hat{e}_b + d\hat{e}_{wr} \tag{12}$$

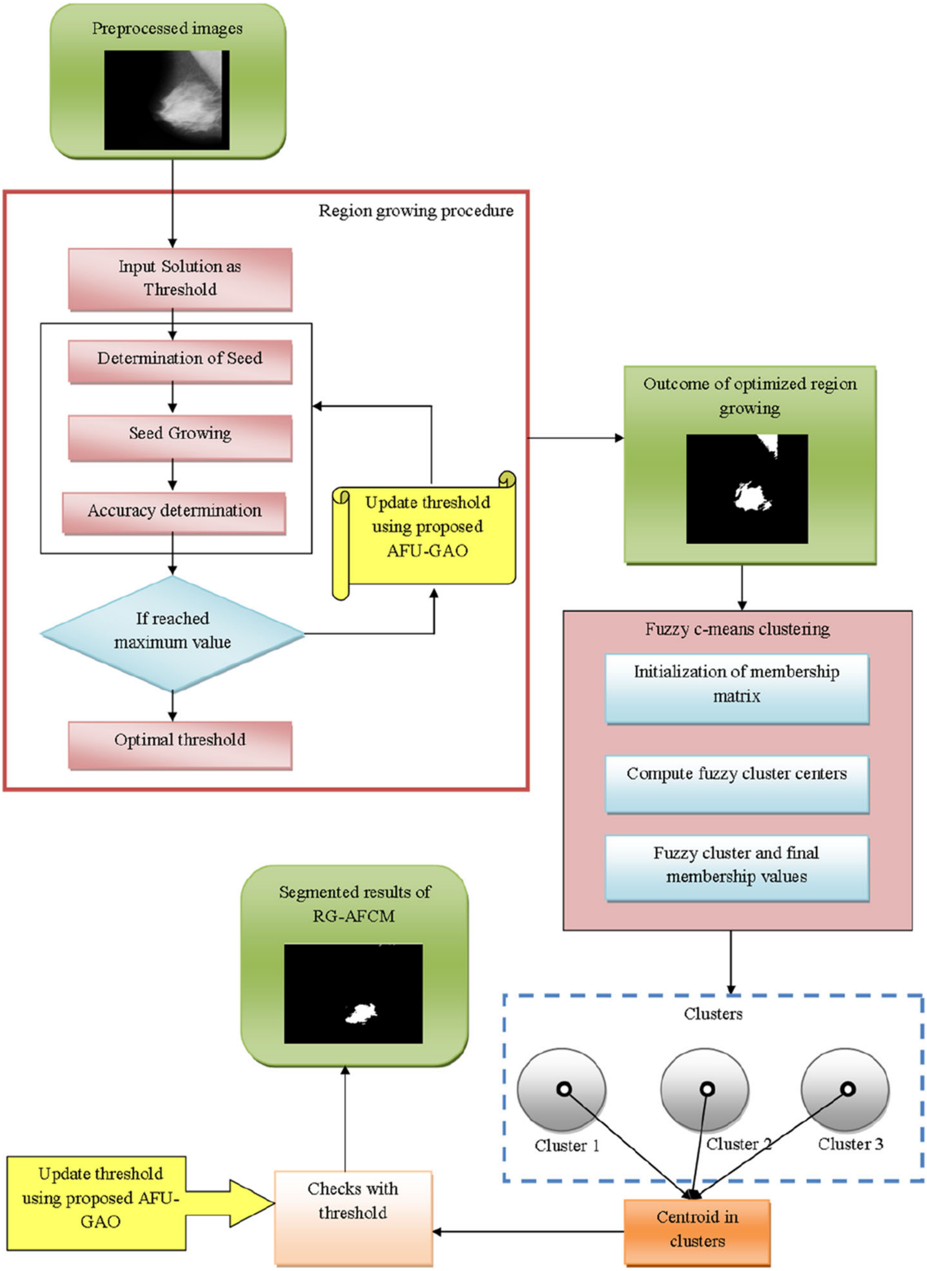

Fig. 3 Proposed RG-AFCM-based segmentation model

This is intended for creating the communication among swarms. It is not employed in the swarm model due to their halt of search space process in the area of a solution from exploring and exploiting. Thus, a new model is formulated for solving the optimization problems, which is given in Eq. (13).

$$A_x^j = h_{dc}\left(\sum_{\substack{y=1\\ y\neq 1}}^{N} h_{dc}\frac{ub_j - lb_j}{2} s\left(\left|a_x^j - a_y^j\right|\right)\frac{a_y - a_x}{a_{xy}}\right) + \overline{K}_j \tag{13}$$

Here, the decreasing coefficient is denoted ash_{dc}that is intended to diminish the mobility of grasshoppers in the region of the goal and also it balances the "exploration and exploitation" of the whole swarm in the region of the goal and to reduce the zones between grasshoppers, the lower bound with J^{th}dimension is denoted as lb_j, the target rate of the J^{th}dimension is termed as $\overline{K}_j$, $ub_j$is the upper bound with J^{th}dimension. As mentioned above, the exploration and exploitation stages are balanced by decreasingh_{dc} that is relation to the number of iteration. Thus, this is derived in Eq. (14).

$$h_{dc} = h_{dc}\max - it\frac{h_{dc}\max - h_{dc}\min}{IT} \tag{14}$$

In Eq. (14), the maximum value is represented as$h_{dc}max$, $h_{dc}min$refers to minimum rate, the maximum number of iterations are noted as$IT$and the current iteration is indicated asit. The values for $h_{dc}max$and $h_{dc}min$ are taken as 1 and 0.00001, respectively. This GOA algorithm has diverse features like more accurate target prediction to get optimal solutions. It also has enhanced global optimization ability, capability of avoiding local optima problem and easy handling of unexpected movement problem. It also enhances the accuracy and tracking efficiency. This method is simple and effective. However, this algorithm suffers from challenges like high computational complexity and less convergence rate. To solve these challenges, a new AFU-GOA algorithm is developed based on the average fitness-based new updating procedure based on distance as given in Eq. (15).

$$d_x = A_{\boldsymbol{best}}^j - A_x^j \tag{15}$$

$$S_x = A_{\boldsymbol{best}}^j - F_1 \times d_x \tag{16}$$

$$A_x^j = S_x \tag{17}$$

Consider the fitness function as $fs(x)$and average fitness as$\boldsymbol{mean}(fs)$. The conventional GOA evaluates the fitness function normally, whereas the proposed AFU-GOA checks fitness function and updates position of the search agent using the fitness function and average fitness. If$fs(x) < \boldsymbol{mean}(fs)$, then the conventional GOA position updating is performed; otherwise the position updating is done by new formula using Eq. (17).

The pseudocode of the proposed AFU-GOA is represented in Algorithm 2.

Algorithm 2: Proposed AFU-GOA

```
Initialization of grasshopper swarm A_x (x = 1,2,3,......, n)
Initialization of b_dc max , b_dc min and I
Estimate the fitness of each search solution
K = the best search solution
While (it < IT)
   for x = 1 : J
      for l = 1 : J
         y = 1 : 2 : J
            if fs(x) < mean(fs)
               for each search solution agent
                  Normalization of distances among the
                  grasshoppers in [1,4]
                  Position update by Eq. (15)
               End for
            else
                  Revise the distance using Eq. (15)
                  Update the social interaction using
                  Eq. (16)
                  Position update by Eq. (17)
            end if
            Bring the current search agent back if it
            goes beyond the boundaries
         end for
      end for
   end for
Revise K if there is a best search solution agent
i = i + 1
End while
Return K
```

Generally, the optimization techniques play an important role in medical image processing because of the huge research among the researchers [11]. These techniques have experienced diverse enhancements in literature that motivates for developing a new model. Meta-heuristic search methodologies are established to be capable and appropriate for numerous applications. The flowchart of the proposed AFU-GOA is specified in Fig. 4.

3.3 Feature extraction

The proposed model uses two feature extraction methods like GLCM and GLRM. After enhanced tumor segmentation process, the features are extracted using these approaches in the proposed breast cancer segmentation and classification model. The segmented images $\boldsymbol{In}_{tm}^{im(seg)}$ are subjected to the feature extraction stage to get significant features.

GLCM [31] is used to compute the spatial relationship of pixels. It also calculates the probability between pixels pairs by some particular values, which helps in the assessment of spatial relationship in an image. The energy is formulated in Eq. (18).

$$Ene = \sum_i \sum_j GL_{ij}^2 \tag{18}$$

Here, the normalized GLCM is represented by GL_{ij}^2 at element$(i,\ j)$. "Entropy, contrast, and homogeneity" are formulated below.

$$Ent = -\sum_i \sum_j GL_{ij} \log_2 GL_{ij} \tag{19}$$

$$Con = \sum_i \sum_j (i-j)^2 GL_{ij} \tag{20}$$

$$\text{Hom} = \sum_i \sum_j \frac{1}{1+(i-j)^2} GL_{ij} \tag{21}$$

Furthermore, the "variance, sum average, and correlation" are equated as follows.

$$\text{V}ar = \sum_i \sum_j (i-\mu)^2 GL_{ij} \tag{22}$$

$$\boldsymbol{SVar} = \sum_{i=2}^{2Cr_{GM}-2} iGL_{ir+\boldsymbol{is}}(i) \tag{23}$$

$$COR = \frac{\sum_i \sum_j (i \times j) GL_{ij} - \mu_{ir}\mu_{\boldsymbol{is}}}{\gamma_{ir}\gamma_{\boldsymbol{is}}} \tag{24}$$

Here, the term μ denotes the mean of GL_{ij} with the amount of grey level in image as Cr_{GM}. The mean and standard deviation of GL_i and GL_j is indicated as μ_{ir}, $\mu_{\boldsymbol{is}}$ and $\gamma_{\boldsymbol{is}}$,$\gamma_{\boldsymbol{is}}$, respectively. Furthermore, the "sum variance, sum entropy, difference entropy, difference variance, and maximum correlation coefficient" are represented as follows.

$$\boldsymbol{Sum}Var = \sum_{i=2}^{2Cr_{GM}} (i - \boldsymbol{SVar})^2 GL_{ir+\boldsymbol{is}}(i) \tag{25}$$

$$\text{S}Ent = \sum_{i=2}^{2Cr_{GM}} GL_{ir+\boldsymbol{is}}(i) \log\{GL_{ir+\boldsymbol{is}}(i)\} \tag{26}$$

$$\text{D}Ent = \sum_{i=0}^{2Cr_{GM}-1} GL_{ir-\boldsymbol{is}}(i) \log\{GL_{ir-\boldsymbol{is}}(i)\} \tag{27}$$

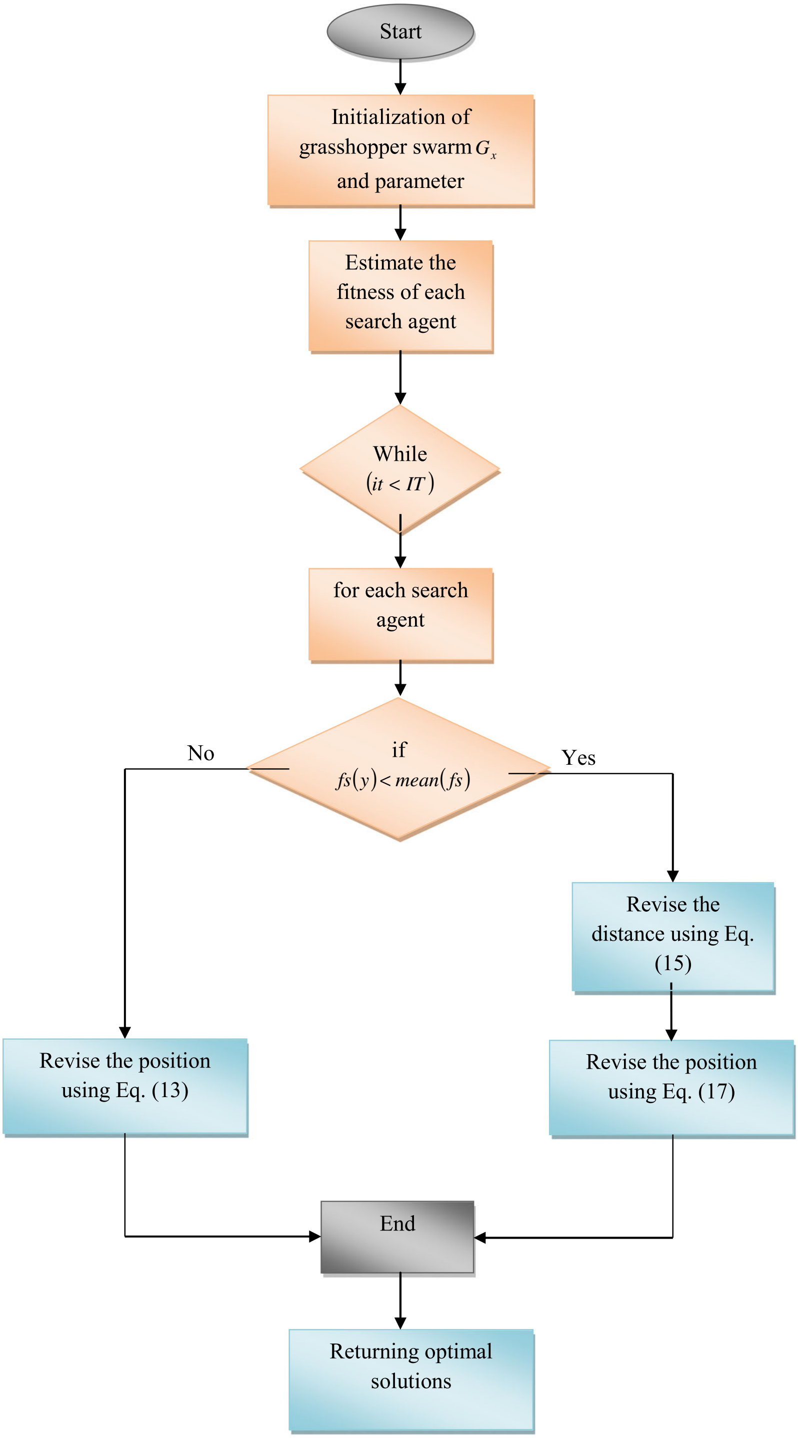

Fig. 4 Flowchart of the proposed AFU-GOA

$$\boldsymbol{DVar} = var\boldsymbol{of}\, GL_{ir-\boldsymbol{is}} \tag{28}$$

$$MCC = \sum_{iw} \frac{GL(i, iw)GL(iv, iw)}{GL_{ir}(i)GL_{\boldsymbol{is}}(iw)} \tag{29}$$

The features extracted by GLCM are denoted as $fe_{fg}^{\boldsymbol{GLCM}}$, where $fg = 1, 2, \ldots, FG$ and FG denotes the total number of features using GLCM method. Further, the GLRM [30] is applied to extract features. GLRM is considered as a matrix, where the texture analysis attains texture features. The statistical data of the higher-order is represented through increasing the intensity of image in GLRM. The computation of "short-run emphasis, long-run emphasis, grey level non-uniformity, run-length non-uniformity, run percentage, (Low Grey Level Run Emphasis)LGRE, (High Grey Level Run Emphasis)HGRE" are formulated in Eq. (30) to Eq. (36), respectively.

$$Sr^{EM} = \frac{1}{nr} \sum_{ur,vr} \frac{Hw(ur, vr)}{vr^2} \tag{30}$$

$$Lr^{EM} = \frac{1}{nr} \sum_{ur,vr} vr^2 Hw(ur, vr) \tag{31}$$

$$Gnu^{NU} = \frac{1}{nr} \sum_{ur} \left(\sum_{vr} Hw(ur, vr)^2 \right) \tag{32}$$

$$Run^{NU} = \frac{1}{nr} \sum_{ur} \left(\sum_{ur} Hw(ur, vr)^2 \right) \tag{33}$$

$$Run^{PER} = \sum_{ur,vr} \frac{nr_{ta}}{Hw(ur, vr)vr} \tag{34}$$

$$\boldsymbol{LGRE}^{EM} = \frac{1}{nr} \sum_{ur,vr} \frac{Hw(ur, vr)}{ur^2} \tag{35}$$

$$\boldsymbol{HGRE}^{EM} = \frac{1}{nr} \sum_{ur,vr} ur^2 Hw(ur, vr) \tag{36}$$

By considering the abovementioned equations, the second-order joint conditional probability density function is indicated by $Hw(ur, vr)$. The GLRM features are termed as $fe_{fn}^{\boldsymbol{GLRM}}$, where $fn = 1, 2, \ldots, FN$ and FN show the total number of features using GLCM method. Consequently, the integration of attained GLCM and GLRM features are denoted asFE_{fe}, where$fe = 1, 2, \cdots, FY$and the total amount of features is denoted asFY. The extracted features$FE_{fe}$are subjected to the classification stage.

4 AFU-GOA-trained recurrent neural network for mammogram image classification

4.1 Objective model for proposed breast cancer diagnosis

This proposed breast cancer diagnosis model mainly focuses on segmentation and classification stages for attaining a more precise and accurate performance. It considers two objectives in the following two phases. The optimized segmentation and classification approaches have been suggested in this model to overcome the challenges of the existing model. The optimization of significant parameters in each technique is performed through the optimization algorithm for getting the optimal solutions. Here, the trial and error method is used for assigning the range for particular constraints, where the range is decided based on the optimal solutions attained in the training phase.

a) Maximization of Segmentation accuracy: The proposed AFU-GOA-RG-AFCM aims to increase the segmentation accuracy by optimizing the threshold. Here, the threshold tuning is adopted in both region growing and FCM-based clustering. Both the threshold values are optimized by the AFU-GOA with the intention of reaching the maximized segmentation accuracy when correlating with the ground truth images. The solution encoding of the proposed breast cancer detection model is given in Fig. 5.

Here, the termThr_{RG}denotes the threshold value in RG, $Thr_{\boldsymbol{AFCM}}$indicates the assigned threshold value in AFCM. The limit of threshold in both RG and AFCM is in the range of 5 to 200. The major objective of this proposed model is headed for increasing the segmentation accuracy, which is given in Eq. (37).

$$fs_1 = \{Thr_{RG}, Thr_{\boldsymbol{AFCM}}\} argmax(Acr) \tag{37}$$

Accuracy $Acr$is defined as "to how closely the measured value of a quantity corresponds to its "true" value". It is formulated in Eq. (38).

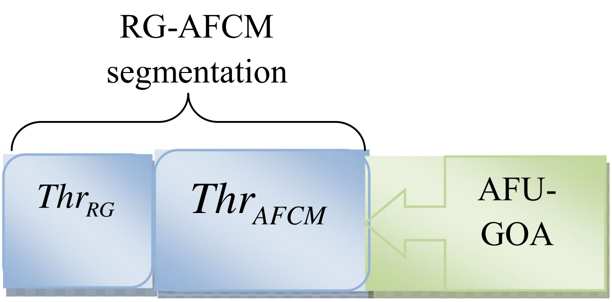

Fig. 5 Solution encoding of the proposed segmentation stage

$$Acr = \frac{\left(tr_{po} + tr_{ng}\right)}{\left(tr_{po} + tr_{ng} + fa_{po} + fa_{ng}\right)} \tag{38}$$

Here, the term tr_{ng} indicates true negatives, tr_{po} denotes true positives, fa_{ng} specifies false negatives fa_{po} referred to as false positives.

b) Minimization of Detection Error: The proposed breast cancer detection model uses the optimal trained RNN for improvising the performance of classification. The training algorithm of RNN is enhanced by AFU-GOA, in which the training weight is optimized in such a way that the error distinction among the measured and the target outcome should attain minimum. RNN algorithm is improved by the AFU-GOA algorithm, in which the weight can be optimized based on the range of 0–1 for efficient detection of breast cancer lesions at an earlier stage in an accurate manner. The solution encoding of the proposed classification stage is depicted in Fig. 6.

The term WT_{fe} is denoted as the weight of RNN. The objective function of the proposed classification based on optimal trained RNN is given in Eq. (39).

$$fs_2 = \left\{WT_{fe}\right\} argmin\left(Err_{\det}\right) \tag{39}$$

The error $Err_{\det}$ among actual Ac_{op} and predicted output $\boldsymbol{pred}_{op}$ has to be minimized in the classification stage that is formulated in Eq. (40).

$$Err_{\det} = Ac_{op} - \boldsymbol{pred}_{op} \tag{40}$$

4.2 AFU-GOA-trained RNN

The developed AFU-GOA-trained RNN [18] classifies the extracted features as normal, malignant and benign. Here, the weight of RNN is updated using proposed AFU-GOA. RNN is a type of ANN, in which the links between the nodes generate a directed graph through a development of information. The steps to design RNN architecture are listed given below. Initially, it examines a simple pre-trained image classification network in Deep Network Designer(DNS). The next step is to prepare a network for transfer learning by editing it in DNS. Transfer learning is the process of taking a pre-trained deep learning network and

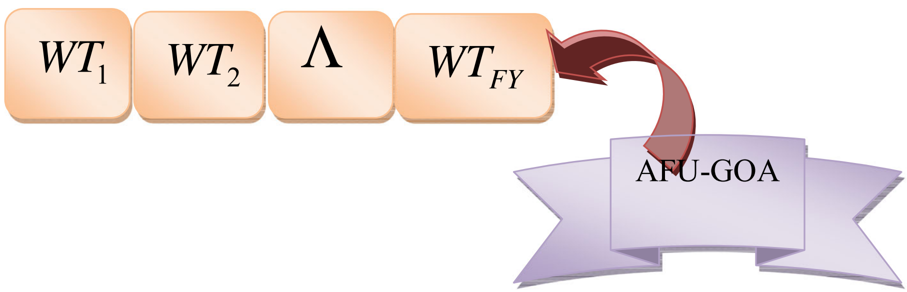

Fig. 6 Solution encoding of the proposed classification model

fine-tuning it to learn a new task. On the Designer pane, select a layer for finalizing the properties. Then to add the layers from the to a network in DNS. The next step is to import data for training, where DNS supports the import of image data and data storing objects. Select an import method based on the type of task. Using DNS, to train a network using image data or any datastore object that works with the train network function. Finally, it exports the network architecture created in DNS to the workspace or Simulink and generates code to recreate the network and training.

One category of RNN is LSTM, which includes a memory cell unit. Furthermore, it consists of three gate units such as "input, forget, and output gates". The use of LSTM (Long Short-Term Memory) is to control the flow and mixing of inputs as per trained Weights. It brings more flexibility in controlling the outputs. LSTM is employed for resolving the explosion and gradient mass. LSTM eliminates the redundant data and achieves the necessary data in series while updating the memory cell unit's state with the abovementioned three gates. (Gate Recurrent Unit)GRU is proposed as a special type of LSTM, which merges the output and forgets gates into a unique update gate termedUg_{in}, where the linear interpolation helps to achieve the current outcome. Assume, $gn_{in} \leftarrow Fe_{fe}$is the $\boldsymbol{in}^{th}$input feature, and $hs_{in-1}$is the earlier hidden state. The updated gate and the reset gate are represented in Eq. (41) and Eq. (42), respectively.

$$Ug_{in} = Af\left(WT^{gnUg} gn_{in} + WT^{hsUg} hs_{in-1}\right) \tag{41}$$

$$Rg_{in} = Af\left(WT^{gnRg} gn_{in} + WT^{hsRg} hs_{in-1}\right) \tag{42}$$

Here, the activation function is termed asAfthat is a logistic sigmoid function. The weight matrix is denoted by$WT_{fe} = \{WT^{gnUg}, WT^{hsUg}, WT^{gnRg}, WT^{hsRg}\}$, which has to be updated to minimize the fault discrepancy between the predicted and actual output. The candidate state of the hidden unit is computed in Eq. (43)

$$\hbar s_{in} = \tan\left(WT^{gnhs} gn_{in} + WT^{hshs}(hs_{in-1} \otimes Rg_{in})\right) \tag{43}$$

In Eq. (43), the element-wise multiplication is represented as$\otimes$, the linear interpolation between $hs_{in-1}$and candidate state $\hbar s_{in}$is referred to as $\boldsymbol{in}^{th}$hidden activation function $hs_{in}$of GRU that is formulated in Eq. (44).

$$\begin{aligned} hs_{in} &= (1 - Ug_{in}) \otimes \hbar s_{in} + Ug_{in} \otimes hs_{in-1} hs_{in} \\ &= (1 - Ug_{in}) \otimes \hbar s_{in} + Ug_{in} \otimes hs_{in-1} \end{aligned} \tag{44}$$

Here, the proposed AFU-GOA optimizes WT_{fe}in RNN and attains the three classes like normal, benign, and malignant types from the input mammogram images. The proposed AFU-GOA-Trained RNN is illustrated in Fig. 7. The number of parameters for RNN is listed as 4 and also the initial input can be considered as the extracted features and the output is normal, benign, malignant. The types of layers are given by the input layer and feed-forward fully connected layer.

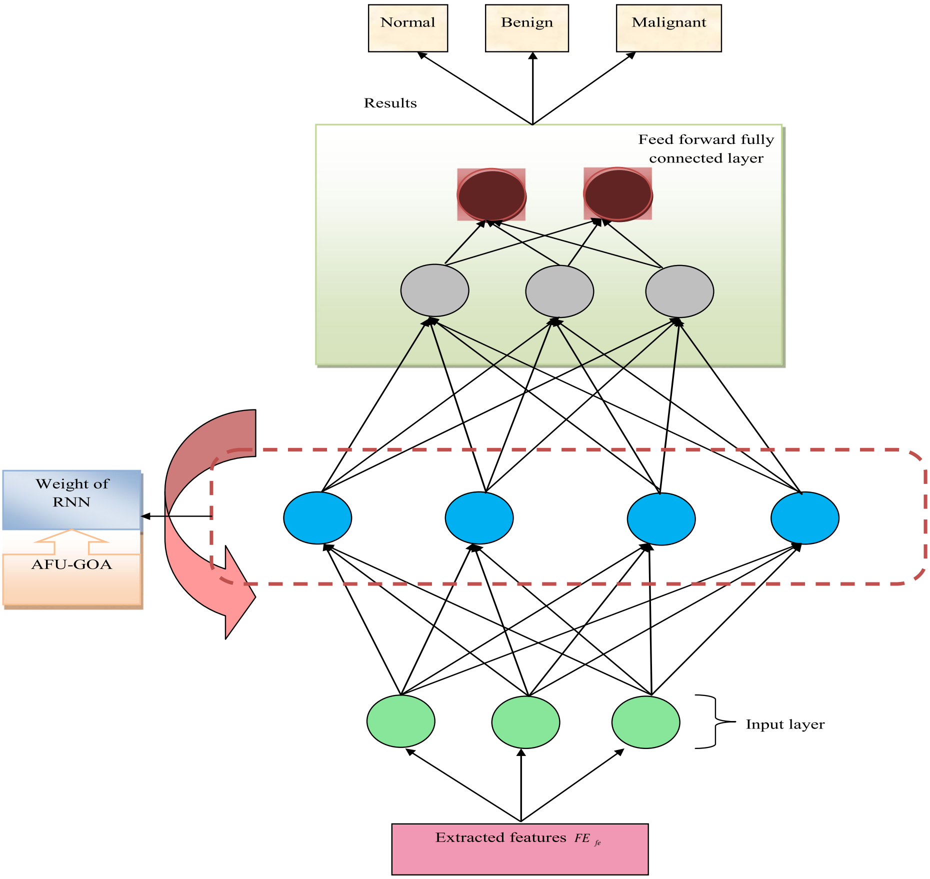

Fig. 7 Proposed AFU-GOA-Trained RNN

5 Results and discussions

5.1 Experimental setup

The proposed breast cancer detection system was executed in MATLAB 2019, and the performance examination was performed. The performance analysis was done by Type I, and Type II measures. The experimental results acquired from the proposed model were compared over the conventional techniques through validation with graphs and tabulations. The proposed model has considered the population size and the maximum number of iterations as 10 and 100, respectively. The developed model was compared over optimization techniques like PSO [4], GWO [25], FF [45], and GOA [37]. Similarly, the proposed model was compared by classifiers such as DT [29], SVM [26], DNN [12], NN [9] and RNN [18]. Likewise, the proposed AFU-GOA-RG-AFCM model was also analyzed with diverse conventional segmentation methods such as Circle Hough [40], active contour [41], Region growing [32], Optimized region growing [31], and Fuzzy set [36]. The Complexity analysis of the proposed approach is compared with other approaches in terms of consumed memory as listed given below. For the firefly algorithm, the time complexity and memory are obtained through $O(it * pop)$ and $\Omega([2 * pop * cl] + [2 * cl] + [2 * it] + pop + 7)$. For the PSO algorithm, the time complexity and memory are obtained through $O(it + (it * pop * cl))$ and$\Omega(4 * pop * cl) + [2 * cl] + [2 * it] + pop + 9$. For the GWO algorithm, the time complexity and memory are obtained through $O(it * pop * cl)$ and $\Omega([2 * pop * cl] + [7 * cl] + [1 * it] + [1 * pop] + 16)$. In our proposed AFU-GOA-RG-AFCM model the time complexity and memory are obtained through $O(2 * pop + (\boldsymbol{Maxit} * ([pop * cl * pop] + pop)))$ and $\Omega([5 * pop * cl] + [2 * cl] + \boldsymbol{Maxit} + [2 * pop] + 7)$. The parameters used in our proposed model are given by, for DNN the hidden neuron count has been considered as 30. For NN the hidden neuron count has been considered as 10. For SVM the kernel function can be considered as Gaussian. Chromosome length is described as the number of optimization values. The evaluation of sample simulation images by different feature extraction techniques have listed in Table 2.

5.2 Performance measures

There are diverse performance measures considered for validating the performance of the proposed model that is explained below.

(a) Sensitivity: “the ratio among true positive and false negatives”.

$$Se = \frac{tr_{po}}{tr_{po} + fa_{ng}} \tag{45}$$

(b) Specificity: “the true negative rate or the proportion of negatives that are correctly identified”.

Table 2 The evaluation for sample simulation images by different feature extraction techniques

Terms	Image1	Image2	Image3	Image4
“Energy”	0.89535	0.89077	0.91143	0.95389
“Entropy”	0.28988	0.3022	0.27567	0.1601
“Contrast”	0.2004	0.18128	0.14782	0.095864
“homogeneity”	0.99082	0.99237	0.99162	0.99481
“Sum Average”	2.5649	2.661	2.4264	2.226
“Correlation”	0.93359	0.95265	0.92894	0.91894
“Sum Variance”	11.053	13.093	8.6825	6.5597
“Sum Entropy”	0.28056	0.29081	0.26505	0.15466
“Difference Entropy”	0.083788	0.077767	0.085554	0.055945
“Difference Variance”	0.2004	0.18128	0.14782	0.095864
“Maximum Correlation Coefficient”	0.93359	0.95265	0.92894	0.91894
“Short Run Emphasis”	0.18428	0.28555	0.25258	0.14384
“Long Run Emphasis”	12,777	12,336	11,980	21,648
“Grey Level Non Uniformity”	265.88	218.18	210.79	189.18
“Run Length Non Uniformity”	70.082	105.09	104.32	85.17
“Run Percentage”	0.015139	0.015762	0.016567	0.010366
“LGRE”	0.4033	0.35781	0.3457	0.46934
“HGRE”	135.66	133.17	112.6	97.428

$$Sp = \frac{tr_{ng}}{fa_{ng}} \tag{46}$$

(c) Precision: "the positive predictive value or the fraction of the positive predictions that are actually positive".

$$Ps = \frac{tr_{po}}{tr_{po} + fa_{po}} \tag{47}$$

(d) (False Positive Rate)FPR: "the ratio of number of false positive predictions to the whole amount of negative predictions".

$$FPR = \frac{fa_{po}}{fa_{po} + tr_{ng}} \tag{48}$$

(e) (False-Negative Rate)FNR: "the proportion of positives that attain negative test results with the test".

$$FNR = \frac{fa_{ng}}{tr_{ng} + tr_{po}} \tag{49}$$

(f) (Negative Predictive Value)NPV: "the difference between the present value of cash inflows and the present value of cash outflows over a period of time."

$$NPV = \frac{fa_{ng}}{fa_{ng} + fa_{po}} \tag{50}$$

(g) (False Discovery Rate)FDR: "a method of conceptualizing the rate of type I errors in null hypothesis testing when conducting multiple comparisons".

$$FDR = \frac{fa_{po}}{fa_{po} + tr_{po}} \tag{51}$$

(h) F1 score: "the weighted average of Precision and Sensitivity".

$$F1 - \boldsymbol{score} = \frac{Sp \cdot Ps}{Ps + Sp} \tag{52}$$

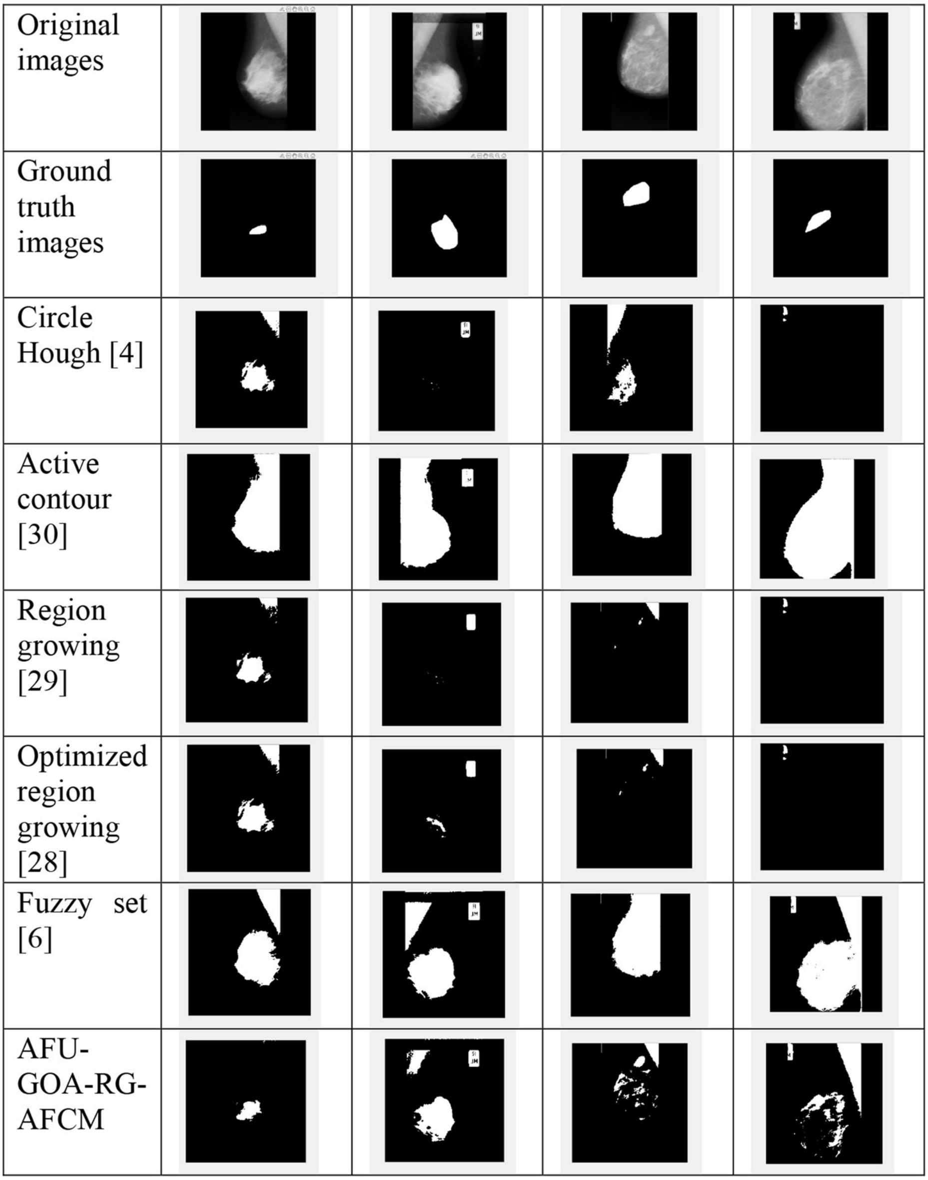

Fig. 8 Sample simulation images of proposed and conventional segmentation models

(i) MCC: "it is estimated by four values".

$$MCC = \frac{tr_{po} \times tr_{ng} - fa_{po} \times fa_{ng}}{\sqrt{\left(tr_{po} + fa_{po}\right)\left(tr_{po} + fa_{ng}\right)\left(fa_{ng} + fa_{po}\right)\left(tr_{po} + fa_{ng}\right)}} \tag{53}$$

Table 3 Segmentation analysis of the proposed and conventional segmentation techniques for breast cancer detection

Measures	Circle Hough [40]	Active contour [41]	Region growing [32]	Optimized region growing [31]	Fuzzy set [36]	AFU-GOA-RG-AFCM
"Accuracy"	0.91374	0.71278	0.92823	0.92346	0.81333	0.99801
"Sensitivity"	0.4835	0.97355	0.21369	0.26073	0.81804	0.91198
"Specificity"	0.9235	0.70686	0.94445	0.93851	0.81323	1
"Precision"	0.12549	0.070111	0.080323	0.087804	0.090442	1
"FPR"	0.076497	0.29314	0.055545	0.061494	0.18677	0
"FNR"	0.5165	0.026452	0.78631	0.73927	0.18196	0.088022
"NPV"	0.9235	0.70686	0.94445	0.93851	0.81323	1
"FDR"	0.87451	0.92989	0.91968	0.9122	0.90956	0
"F1-Score"	0.19926	0.1308	0.11676	0.13137	0.16288	0.95396
"MCC"	0.21441	0.21709	0.098837	0.11829	0.23217	0.95401

5.3 Segmentation results

The proposed model contributes the segmentation as the major concept for mammogram images using RG-AFCM, which are compared with diverse conventional segmentation approaches. The sample images for the proposed as well as various traditional segmentation methods are listed in Fig. 8.

5.4 Segmentation analysis

The proposed model utilizes segmentation as the major contribution, which is done by AFU-GOA-RG-AFCM that is compared with traditional segmentation approaches and heuristic-based models as represented in Tables 3 and 4, respectively. The accuracy of the proposed AFU-GOA-RG-AFCM is 9%, 40%, 7.5%, 8%, and 22.7% enhanced than Circle Hough, Active contour, Region growing, Optimized region growing and Fuzzy set, respectively. The specificity of the developed AFU-GOA-RG-AFCM is 8%, 41%, 5.8%, 6.5%, and 22.9% superior to Circle Hough, Active contour, Region growing, Optimized region growing and Fuzzy set, respectively. The FNR of the suggested AFU-GOA-RG-AFCM is 82%, 69%, 88.8%, 88% and 51% improved than Circle Hough, Active contour, Region growing, Optimized region growing and Fuzzy set, respectively. The accuracy of the proposed AFU-GOA-

Table 4 Segmentation analysis of the proposed and conventional heuristic-based techniques for breast cancer segmentation

Measures	FF [45]	PSO [4]	GWO [25]	GOA [37]	AFU-GOA-RG-AFCM
"Accuracy"	0.95833	0.94792	0.95833	0.9375	0.96875
"Sensitivity"	0.84	0.84	0.92	0.84	0.96
"Specificity"	1	0.98592	0.97183	0.97183	0.97183
"Precision"	1	0.95455	0.92	0.91304	0.92308
"FPR"	0	0.014085	0.028169	0.028169	0.028169
"FNR"	0.16	0.16	0.08	0.16	0.04
"NPV"	1	0.98592	0.97183	0.97183	0.97183
"FDR"	0	0.045455	0.08	0.086957	0.076923
"F1-Score"	0.91304	0.89362	0.92	0.875	0.94118
"MCC"	0.89174	0.8624	0.89183	0.83472	0.92024

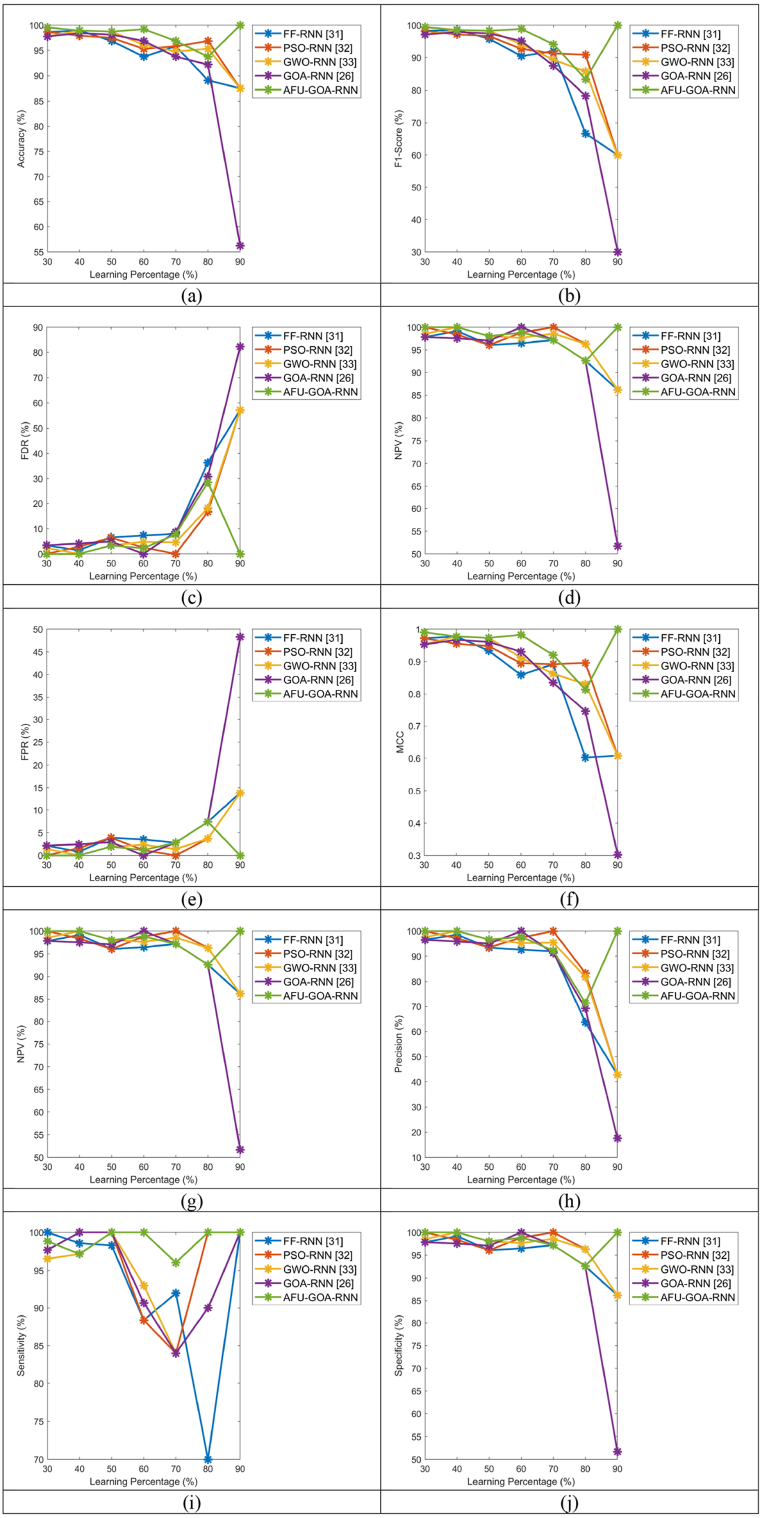

FF-RNN [31]
PSO-RNN [32]
GWO-RNN [33]
GOA-RNN [26]
AFU-GOA-RNN
Accuracy (%)
Learning Percentage (%)
(a)
F1-Score (%)
(b)
FDR (%)
(c)
NPV (%)
(d)
FPR (%)
(e)
MCC
(f)
NPV (%)
(g)
Precision (%)
(h)
Sensitivity (%)
(i)
Specificity (%)
(j)

Fig. 9 Performance analysis of the proposed and conventional heuristic-based algorithms for proposed breast cancer segmentation and classification model in terms of **a** Accuracy, **b** F1-score, **c** FDR, **d** FNR, **e** FPR, **f** MCC, **g** NPV, **h** Precision, **i** Sensitivity and **j** Specificity

RG-AFCM is 1%, 2%, 1% and 3% advanced than FF, PSO, GWO and GOA, respectively. The FNR of the proposed AFU-GOA-RG-AFCM is 75% enhanced than FF, PSO, and GOA, respectively and 50% enhanced than GWO. Therefore, the proposed AFU-GOA-RG-AFCM model performs better than other segmentation approaches.

5.5 Performance analysis in terms of meta-heuristic based algorithms

The performance analysis of the proposed AFU-GOA-trained RNN model is enhanced by comparing diverse algorithms by varying learning percentages, which is represented in Fig. 9. The accuracy of the proposed AFU-GOA-RNN is 13.7%, 13.1%, 12.5% and 76.7% enhanced than FF-RNN, PSO-RNN, GWO-RNN and GOA-RNN, respectively at learning percentage 90. The F1-score of the proposed AFU-GOA-RNN is 62%, 59% and 57% superior to FF-RNN, PSO-RNN, and GWO-RNN, respectively for learning percentage 90. The FDR of the developed AFU-GOA-RNN is 33% minimized than FF-RNN, 20% minimized than PSO-RNN, 42% minimized than GWO-RNN and 50% minimized than GOA-RNN when considering the learning percentage as 50. The FNR of implemented AFU-GOA-RNN for learning percentage as 70 is 37.5% reduced than FF-RNN and 68.75% reduced than PSO-RNN, GWO-RNN and GOA-RNN, respectively. By considering the learning percentage as 50, the FPR of the proposed AFU-GOA-RNN is 60%, 50%, 33% and 42.8% decreased than FF-RNN, PSO-RNN, GWO-RNN and GOA-RNN, respectively. The MCC of the proposed AFU-GOA-RNN is 15%, 8.8%, 6.5% and 3% improved than FF-RNN, PSO-RNN, GWO-RNN and GOA-RNN, respectively at learning percentage 60. The NPV of the implemented AFU-GOA-RNN is 15% better than FF-RNN, 13% better than PSO-RNN, 12.5% better than GWO-RNN and 86.7% better than GOA-RNN by considering the learning percentage as 90. The precision for learning percentage 80 is 10% and 2.8% enhanced than FF-RNN and GOA-RNN, respectively. The sensitivity of the proposed AFU-GOA-RNN is 3.7% superior to FF-RNN and 14% superior to PSO-RNN, GWO-RNN and GOA-RNN, respectively for learning percentage 70. The specificity of the developed AFU-GOA-RNN is 1%, 1.5%, 3% and 2% increased than FF-RNN, PSO-RNN, GWO-RNN and GOA-RNN, respectively by considering learning percentage 70. Therefore, the proposed AFU-GOA-based RNN model improves the performance than conventional models.

5.6 Performance analysis on diverse machine learning algorithms

The performance of the proposed AFU-GOA-RNN is compared with various classifiers in terms of diverse performance measures that is represented in Fig. 10. The accuracy of the proposed AFU-GOA-RNN is 23.7%, 2%, 32%, and 11% superior to RNN, DNN, DT and NN, respectively for learning percentage 90. The F1-score of the proposed AFU-GOA-RNN is 4.2%, 15%, 22.5%, 8.8% and 63% improved than RNN, DNN, DT, NN and SVM, respectively at learning percentage 60. The FDR of the developed AFU-GOA-RNN is 88%, 60%, 90%, 84% and 91% minimized than RNN, DNN, DT, NN and SVM, respectively for learning percentage 90. The FNR of the proposed AFU-GOA-RNN on considering the learning percentage 70 is 58%, 50%, 66%, 77% and 75% reduced than RNN, DNN, DT, NN and SVM, respectively. When considering the learning

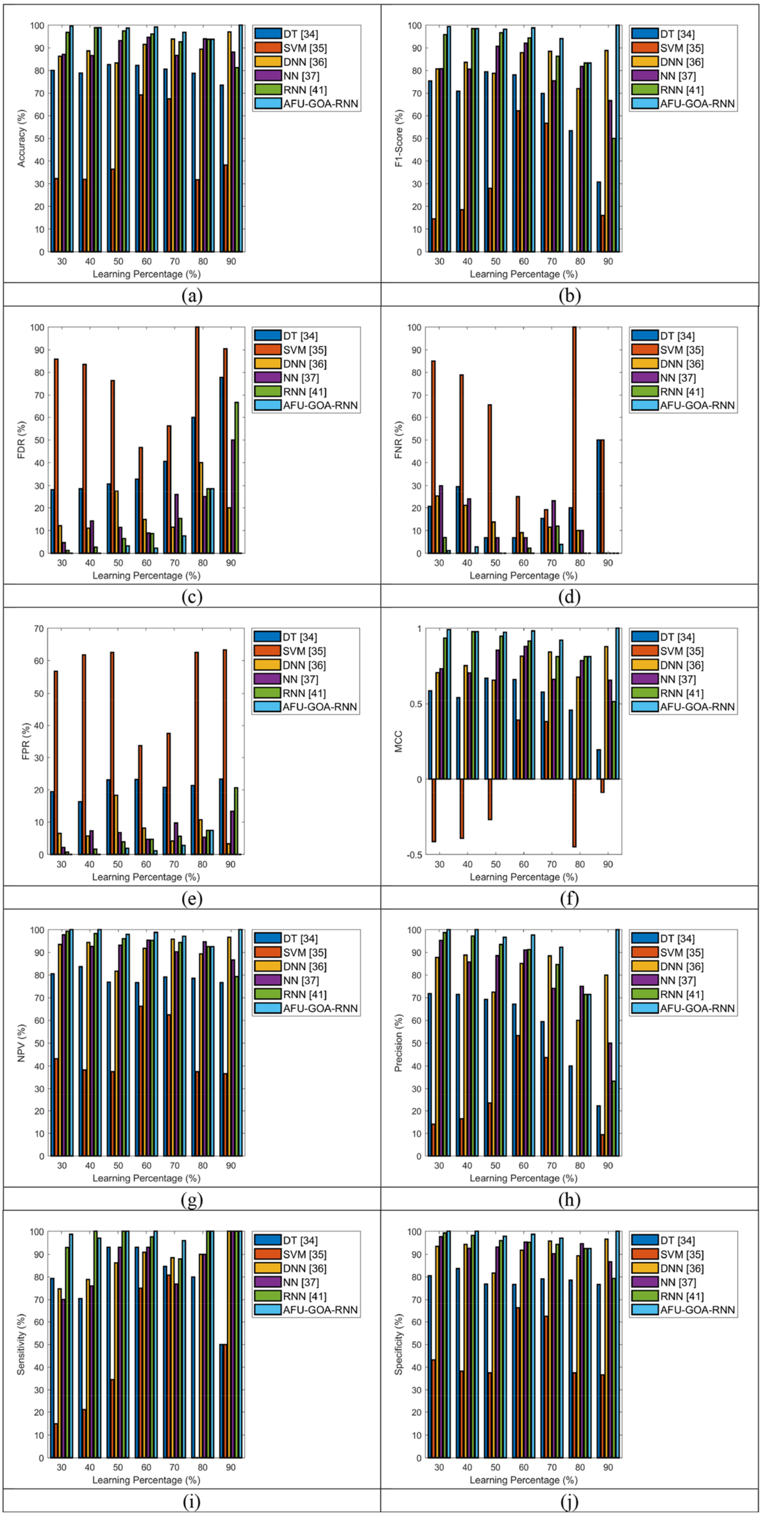

DT [34]
SVM [35]
DNN [36]
NN [37]
RNN [41]
AFU-GOA-RNN
Accuracy (%)
F1-Score (%)
FDR (%)
FNR (%)
FPR (%)
MCC
NPV (%)
Precision (%)
Sensitivity (%)
Specificity (%)
Learning Percentage (%)
30 40 50 60 70 80 90
(a)
(b)
(c)
(d)
(e)
(f)
(g)
(h)
(i)
(j)

Fig. 10 Performance analysis of the proposed and conventional classifiers for proposed breast cancer segmentation and classification model in terms of **a** Accuracy, **b** F1-score, **c** FDR, **d** FNR, **e** FPR, **f** MCC, **g** NPV, **h** Precision, **i** Sensitivity and **j** Specificity

percentage 70, the FPR of the proposed AFU-GOA-RNN is 37.5% diminished than RNN, 16% diminished than DNN, 75% diminished than DT, 50% diminished than NN and 85% diminished than SVM. On considering the learning percentage as 70, the MCC of the proposed AFU-GOA-RNN is 3.6% enhanced than RNN, 4.9% enhanced than DNN, 41% enhanced than DT and 21% enhanced than NN. The NPV of the suggested AFU-GOA-RNN is 3%, 6.5%, 30%, 5.9% and 50% advanced than RNN, DNN, DT, NN and SVM, respectively at learning percentage 60. The precision is 5.8%, 3.4%, 50% and 25% progressed than RNN, DNN, DT and NN, respectively for learning percentage 70. The sensitivity of the proposed AFU-GOA-RNN by considering the learning percentage as 70 is 10%, 9.3%, 14.6%, 25% and 17.5% better than RNN, DNN, DT, NN and SVM, respectively. The specificity of the designed AFU-GOA-RNN is 2%, 22.5%, 30%, and 4% improved than RNN, DNN, DT and NN, respectively at learning percentage 50. As a result, the proposed model in terms of classification is outperformed the traditional models.

5.7 Overall performance analysis

The overall performance analysis of the proposed model compared with diverse heuristic based algorithms and numerous classifiers are represented in Tables 5 and 6 respectively. The accuracy of the developed AFU-GOA-RNN is 1%, 2%, 1% and 3% enhanced than PSO-RNN, GWO-RNN, FF-RNN and GOA-RNN. Similarly, the accuracy of the proposed AFU-GOA-RNN is 20%, 43%, 3%, 11% and 4% better than DT, SVM, DNN, NN and RNN, respectively. Hence, the proposed classification using AFU-GOA-based trained RNN establishes the better performance than existing models.

5.8 State of art comparison for different algorithms

The state of art comparison for different heuristic-based algorithms has been shown in Table 7. The precision of the developed AFU-GOA-RNN is 48.843%, 47.4748%, and 47.7012% enhanced than DL-CNN, ENSEMBLE LEARNING, and DLA-EABA. Hence, the proposed classification using AFU-GOA-based trained RNN attained better performance than existing models.

Table 5 Evaluating proposed and traditional heuristic-based breast cancer detection model

Measures	PSO-RNN [4]	GWO-RNN [25]	FF-RNN [45]	GOA-RNN [37]	AFU-GOA-RNN
"Accuracy"	0.95833	0.94792	0.95833	0.9375	0.96875
"Sensitivity"	0.84	0.84	0.92	0.84	0.96
"Specificity"	1	0.98592	0.97183	0.97183	0.97183
"Precision"	1	0.95455	0.92	0.91304	0.92308
"FPR"	0	0.014085	0.028169	0.028169	0.028169
"FNR"	0.16	0.16	0.08	0.16	0.04
"NPV"	1	0.98592	0.97183	0.97183	0.97183
"FDR"	0	0.045455	0.08	0.086957	0.076923
"F1-Score"	0.91304	0.89362	0.92	0.875	0.94118
"MCC"	0.89174	0.8624	0.89183	0.83472	0.92024

Table 6 Evaluating proposed and traditional machine learning breast cancer detection model

Measures	DT [29]	SVM [26]	DNN [12]	NN [9]	RNN [18]	AFU-GOA-RNN
"Accuracy"	0.80612	0.67347	0.93878	0.86735	0.92708	0.96875
"Sensitivity"	0.84615	0.80769	0.88462	0.76923	0.88	0.96
"Specificity"	0.79167	0.625	0.95833	0.90278	0.94366	0.97183
"Precision"	0.59459	0.4375	0.88462	0.74074	0.84615	0.92308
"FPR"	0.20833	0.375	0.041667	0.097222	0.056338	0.028169
"FNR"	0.15385	0.19231	0.11538	0.23077	0.12	0.04
"NPV"	0.79167	0.625	0.95833	0.90278	0.94366	0.97183
"FDR"	0.40541	0.5625	0.11538	0.25926	0.15385	0.076923
"F1-Score"	0.69841	0.56757	0.88462	0.75472	0.86275	0.94118
"MCC"	0.58088	0.38214	0.84295	0.66407	0.81342	0.92024

5.9 Statistical analysis on the accurateness

Statistical measures are used to collect the data, employ the correct analyses, and effectively present the results. It is a major process of making decisions based on data and making predictions. The Statistical metrics on sample images for the proposed breast cancer segmentation and classification model have been represented in Fig. 11. The given graph proves that the accuracy of the proposed AFU-GOA-RNN model is improved than the other conventional algorithms.

5.10 Analysis on computation time

The Complexity analysis of the proposed approach in terms of consumed time has been shown in Table 8. Hence, it is proved that from the given Table 7 and the computation time is lower than the other different heuristic algorithms.

6 Results and discussion

The main advantages of the proposed AFU-GOA-RNN model are enhanced global optimization ability, the capability of avoiding local optima problems, and easy handling of unexpected movement problems. It also enhances accuracy and tracking efficiency. This method is simple and effective. Due to these advantages, the proposed AFU-GOA-RNN performs better than the existing

Table 7 State of art comparison for different heuristic algorithms for breast cancer detection model

TERMS	DL-CNN [7]	ENSEMBLE LERNING [24]	DLA-EABA [47]	AFU-GOA-RNN
"Accuracy"	0.94444	0.93556	0.96	0.96875
"Sensitivity"	0.73913	0.57143	0.82353	0.96
"Specificity"	0.9555	0.95972	0.96536	0.97183
"Precision"	0.47222	0.48485	0.48276	0.92308
"FPR"	0.044496	0.040284	0.034642	0.028169
"FNR"	0.26087	0.42857	0.17647	0.04
"NPV"	0.9555	0.95972	0.96536	0.97183
"FDR"	0.52778	0.51515	0.51724	0.076923
"F1-Score"	0.57627	0.52459	0.6087	0.94118
"MCC"	0.56387	0.49218	0.61255	0.92024

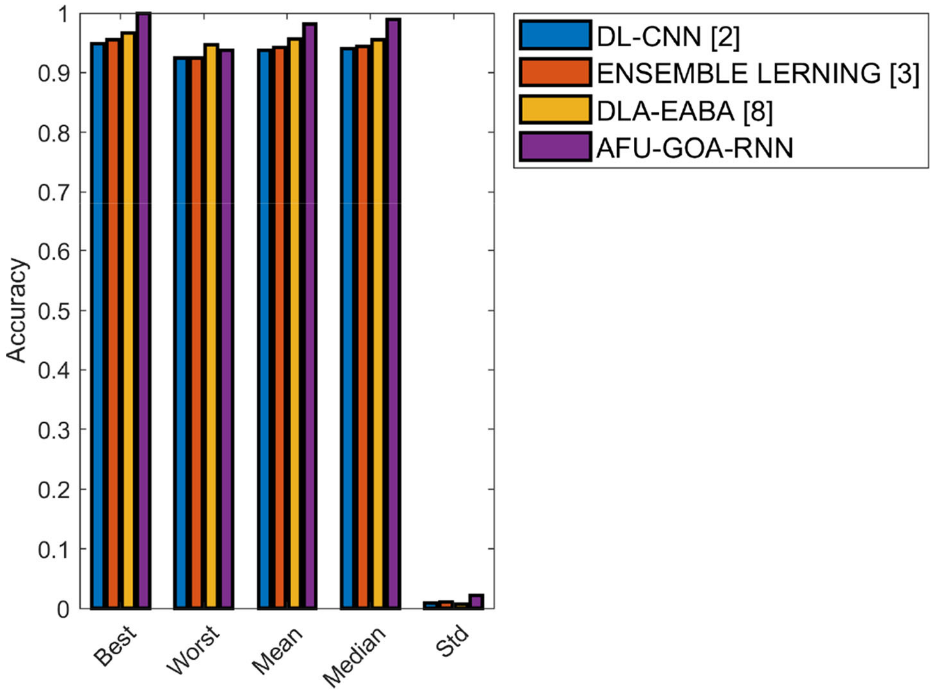

Fig. 11 Statistical metrics on sample images for proposed breast cancer segmentation and classification model

methods. Thus, the outcomes of performance analysis are better with the AFU-GOA-RNN model than the other methods for breast cancer detection model. The failure case of the proposed AFU-GOA-RNN includes, it can handle some hard and challenging, large-scale optimization problems and less convergence rate. Therefore, this performance degradation can be solved in the future by utilizing intelligent approaches like hybrid classifiers or ensemble learning with heuristic improvement and also mainly focused on the error analysis of the proposed model.

7 Conclusion

This paper has developed a new mammography segmentation and classification model. The collected images were initially preprocessed that were segmented using a new enhanced tumor segmentation approach termed RG-AFCM, in which threshold values were optimized using AFU-GOA. Furthermore, the segmented images were performed with feature extraction, in which the features were extracted by GLCM and GLRM methods. In addition, the extracted features were classified using AFU-GOA-trained RNN. Here, a new AFU-GOA technique was developed to enhance the accuracy of segmentation and classification stages. From the

Table 8 State of art comparison for different heuristic algorithms for breast cancer detection model in terms of computational time

Terms	PSO.RNN [4]	GWO.RNN [25]	FF.RNN [45]	GOA.RNN [37]	AFU-GOA-RNN
"TIME"	1409.2	904.31	1177.6	991.17	679.97

experimentation results, the accuracy of the implemented AFU-GOA-RG-AFCM was 9% better than Circle Hough, 40% better than Active contour, 7.5% better than Region growing, 8% better than optimized region growing, and 22.7% better than Fuzzy set. Similarly, the accuracy of the proposed AFU-GOA-RNN was 23.7% superior to RNN, 2% superior to DNN, 32% superior to DT, and 11% superior to NN for learning percentage 90. Therefore, the proposed model has performed better than other conventional models for accurate breast cancer detection. The result of statistical metrics on sample images for the proposed breast cancer segmentation and classification model has proved that the accuracy has been improved and also the computation time is better than the other different heuristic algorithms.

Declarations

Conflict of interest The authors declare no conflict of interest.

References

1. Adhikari SK, Sing JK, Basu DK, Nasipuri M (2015) Conditional spatial fuzzy C-means clustering algorithm for segmentation of MRI images. Appl Soft Comput 34:758–769
2. Ashraf AB, Gavenonis SC, Daye D, Mies C, Rosen MA, Kontos D (2013) A multichannel Markov random field framework for tumor segmentation with an application to classification of gene expression-based breast Cancer recurrence risk. IEEE Trans Med Imaging 32(4):637–648
3. Been Lim H, Nhung NTT, Li E-P, Duc Thang N (2008) Confocal microwave imaging for breast Cancer detection: delay-multiply-and-sum image reconstruction algorithm. IEEE Trans Biomed Eng 55(6):1697–1704
4. Bonyadi MR, Michalewicz Z (2016) Analysis of stability, local convergence, and transformation sensitivity of a variant of the particle swarm optimization algorithm. IEEE Trans Evol Comput 20(3):370–385
5. Chemtex RM, Kantheti S, Kantheti S (2020) Classification of Skin cancer using deep learning, Convolutional Neural Networks -Opportunities and vulnerabilities- A systematic Review. Int J Modern Trends Sci Technol 6(11):101–108
6. Dheeba J, Albert Singh N, Tamil Selvi S (2014) Computer-aided detection of breast cancer on mammograms: a swarm intelligence optimized wavelet neural network approach. J Biomed Inform 49:45–52
7. Duraisamy S, Emperumal S (2017) Computer-aided mammogram diagnosis system using deep learning convolutional fully complex-valued relaxation neural network classifier. IET Comput Vis 11(8):656–662
8. Feng X, Song L, Wang S, Song H, Chen H, Liu Y, Lou C, Zhao J, Liu Q, Liu Y, Zhao R, Xing K, Li S, Yu Y, Liu Z, Yin C, Han B, du Y, Xin R, … Zhou F (2019) Accurate prediction of neoadjuvant chemotherapy pathological complete remission (pCR) for the four sub-types of breast cancer. IEEE Access 7:134697–134706
9. Gao X, Liao L (2010) A new one-layer neural network for linear and quadratic programming. IEEE Trans Neural Netw 21(6):918–929
10. Geweid GGN, Abdallah MA (2019) A novel approach for breast Cancer investigation and recognition using M-level set-based optimization functions. IEEE Access 7:136343–136357
11. GhouseBasha TS, Aloysius G, Rajakumar BR, Giri Prasad MN, Sridevi PV (2012) A constructive smart antenna beam-forming technique with spatial diversity. IET Microwaves, Antennas & Propagation 6(7): 773–780
12. Gong M, Liu J, Li H, Cai Q, Su L (2015) A multiobjective sparse feature learning model for deep neural networks. IEEE Trans Neural Netw Learn Syst 26(12):3263–3277
13. Ibrahim A, Mohammed S, Ali HA, Hussein SE (2020) Breast Cancer segmentation from thermal images based on chaotic Salp swarm algorithm. IEEE Access 8:122121–122134
14. Jameel S (2021) Malebary and Arshad Hashmi, "automated breast mass classification system using deep learning and ensemble learning in digital mammogram,". IEEE Access 9:55312–55328
15. Kao T, Boverman G, Kim BS, Isaacson D, Saulnier GJ, Newell JC, Choi MH, Moore RH, Kopans DB (2008) Regional Admittivity spectra with Tomosynthesis images for breast Cancer detection: preliminary patient study. IEEE Trans Med Imaging 27(12):1762–1768

16. Kaura P, Singh G (2019) Parminder Kaur "intellectual detection and validation of automated mammogram breast cancer images by multi-class SVM using deep learning classification," informatics in medicine unlocked. Vol. 16:100239
17. Lee H, Park J, Hwang JY (2020) Channel attention module with multiscale grid average pooling for breast Cancer segmentation in an ultrasound image. IEEE Trans Ultrason Ferroelectr Freq Control 67(7):1344–1353
18. Li F, Liu M (2019) A hybrid Convolutional and Recurrent Neural Network for Hippocampus Analysis in Alzheimer's Disease. J Neurosci Methods 323:108–118
19. Mahmood T, Li J, Pei Y, Akhtar F, Imran A, Rehman KU (2020) A brief survey on breast Cancer diagnostic with deep learning schemes using multi-image modalities. IEEE Access 8:165779–165809
20. Malebary SJ, Hashmi A (2021) Automated breast mass classification system using deep learning and ensemble learning in digital mammogram. IEEE Access 9:55312–55328
21. Malipatil S, Maheshwari V, Chandra MB (2020) Area Optimization of CMOS Full Adder Design Using 3T XOR. International Conference on Wireless Communications Signal Processing and Networking (WiSPNET), pp 192–194
22. Michael E, He M, Li H, Kulwa F, Li J (2021) Breast cancer segmentation methods: current status and future potentials. Biomed Res Int
23. Muduli D, Dash R, Majhi B (2020) Automated breast cancer detection in digital mammograms: a moth flame optimization based ELM approach. Biomedical Signal Processing and Control 59:101912
24. Mugahed A, Al-antari, Kim T-S (2020) Evaluation of deep learning detection and classification towards computer-aided diagnosis of breast lesions in digital X-ray mammograms. Comput Methods Prog Biomed 196:105584
25. Nirmala Sreedharan NP, Ganesan B, Raveendran R, Sarala P, Dennis B, R. Boothalingam R. (2018) Grey wolf optimisation-based feature selection and classification for facial emotion recognition. IET Biometrics 7(5):490–499
26. Ong C, Shao S, Yang J (2010) An improved algorithm for the solution of the regularization path of support vector machine. IEEE Trans Neural Netw 21(3):451–462
27. Pinker K, Perry N, Milner S et al (2010) Accuracy of breast cancer detection with full-field digital mammography and integral computer-aided detection correlated with breast density as assessed by a new automated volumetric breast density measurement system. Breast Cancer Res 12
28. Pramanik S, Ghosh DB, Nasipuri M (2020) Segmentation of breast-region in breast Thermogram using arc-approximation and triangular-space search. IEEE Trans Instrum Meas 69(7):4785–4795
29. Quellec G, Lamard M, Bekri L, Cazuguel G, Roux C, Cochener B (2010) Medical case retrieval from a Committee of Decision Trees. IEEE Trans Inf Technol Biomed 14(5):1227–1235
30. Radhakrishnan M, Kuttiannan T (2012) Comparative Analysis of Feature Extraction Methods for the Classification of Prostate Cancer from TRUS Medical Images. IJCSI International Journal of Computer Science Issues 9(1)
31. Rajeshwari S (2020) Patil and Nagashettappa Biradar "automated mammogram breast cancer detection using the optimized combination of convolutional and recurrent neural network,". Evol Intel
32. Rajeshwari S (2020) Patil and Nagashettappa Biradar, "improved region growing segmentation for breast cancer detection: progression of optimized fuzzy classifier,". International Journal of Intelligent Computing and Cybernetics
33. Roslidar R, Rahman A, Muharar R, Syahputra MR, Arnia F, Syukri M, Pradhan B, Munadi K (2020) A review on recent Progress in thermal imaging and deep learning approaches for breast Cancer detection. IEEE Access 8:116176–116194
34. Saha M, Chakraborty C (2018) Her2Net: a deep framework for semantic segmentation and classification of cell membranes and nuclei in breast Cancer evaluation. IEEE Trans Image Process 27(5):2189–2200
35. Wessam M. Salama, Moustafa H. Aly" Deep learning in mammography images segmentation and classification: Automated CNN approach," Alexandria Engineering Journal, Volume 60, Issue 5, Pages 4701–4709, 2021.
36. Salih AM, Kamil M y (2019) Mammography images segmentation based on fuzzy set and thresholding. Al-Mustansiriyah Journal of Science 29(168)
37. Saremi S, Mirjalili S (2017) Andrew Lewis "grasshopper optimisation algorithm: theory and application,". Adv Eng Softw 105:30–47
38. T. Sathya Priya, and Dr. T. Ramaprabha "Resnet based feature extraction with decision tree classifier for Classificaton of mammogram images," Turkish Journal of Computer and Mathematics Education, Vol.12, No.2, pp. 1147–1153, 2021.
39. Tang J, Rangayyan RM, Xu J, Naqa IE, Yang Y (2009) Computer-aided detection and diagnosis of breast Cancer with mammography: recent advances. IEEE Trans Inf Technol Biomed 13(2):236–251

40. Vijayarajeswari R, Parthasarathy P, Vivekanandan S, Alavudeen Basha A (2019) Classification of mammogram for early detection of breast cancer using SVM classifier and Hough transform. Measurement 146: 800–805
41. Wang Y, Liu L, Zhang H, Cao Z, Lu S (2010) Image segmentation using active contours with normally biased GVF external force. IEEE Signal Processing Letters 17(10):875–878
42. Wang Z, Li M, Wang H, Jiang H, Yao Y, Zhang H, Xin J (2019) Breast Cancer detection using extreme learning machine based on feature fusion with CNN deep features. IEEE Access 7:105146–105158
43. Woten DA, Lusth J, El-Shenawee M (2007) Interpreting artificial neural networks for microwave detection of breast Cancer. IEEE Microwave and Wireless Components Letters 17(12):825–827
44. Xu J, Xiang L, Liu Q, Gilmore H, Wu J, Tang J, Madabhushi A (2016) Stacked sparse autoencoder (SSAE) for nuclei detection on breast Cancer histopathology images. IEEE Trans Med Imaging 35(1):119–130
45. Yang X-S (2013) Multiobjective firefly algorithm for continuous optimization. Eng Comput 29(2):175–184
46. Yap MH, Pons G, Marti J, Ganau S, Sentis M, Zwiggelaar R, Davison AK, Marti R, Moi Hoon Yap, Pons G, Marti J, Ganau S, Sentis M, Zwiggelaar R, Davison AK, Marti R (2018) Automated breast ultrasound lesions detection using convolutional neural networks. IEEE Journal of Biomedical and Health Informatics 22(4):1218–1226
47. Zheng J, Lin D, Gao Z, Wang S, He M, Fan J (2020) Deep learning assisted efficient AdaBoost algorithm for breast Cancer detection and early diagnosis. IEEE Access 8:96946–96954
48. Zhu Y, Huang C (2012) An improved median filtering algorithm for image noise reduction. Phys Procedia 25:609–616

Publisher's note Springer Nature remains neutral with regard to jurisdictional claims in published maps and institutional affiliations.

Affiliations

Rajeshwari S. Patil[1] • Nagashettappa Biradar[2] • Rashmi Pawar[3]

✉ Rajeshwari S. Patil
rspatil1272014@gmail.com

Nagashettappa Biradar
nmbiradar@gmail.com

Rashmi Pawar
rashmi.ajadhav@gmail.com

[1] Department of Electronics & Communication, B.L.D.E.A's V.P.Dr. P.G.H. College of Engg. & Tech (Affiliated to Visvesvaraya Technological University), Vijayapur, India

[2] Department of Electronics & Communication Engineering, Bheemanna Khandre Institute of Technology, Bhalki, India

[3] Department of Electrical and Electronics, B.L.D.E.A's V. P. Dr. P. G. Halakatti College of Engineering and Technology (Affiliated to Visvesvaraya Technological University), Vijayapur, India